

Molecular Structure of a New Lead Titanium Bimetallic Alkoxide Complex, $[\text{PbTi}_2(\mu_4\text{-O})(\text{OOCCH}_3)(\text{OCH}_2\text{CH}_3)_7]_2$: Evolution of Structure on Heat Treatment and the Formation of Thin-Layer Dielectrics

Hee K. Chae, David A. Payne,* Zhengkui Xu, and Linqing Ma

Department of Materials Science and Engineering
Materials Research Laboratory, and
Beckman Institute
University of Illinois at Urbana–Champaign
Urbana, Illinois 61801

Received March 29, 1994

Revised Manuscript Received June 20, 1994

The properties of electrical ceramics are dependent on structure, at both the single crystal and the microstructural level.¹ Common examples of structure types include perovskite (ABO_3) and tungsten bronze (AB_2O_6). For example, BaTiO_3 is a widely used capacitor material, and $(\text{Sr},\text{Ba})\text{Nb}_2\text{O}_6$ finds applications in pyroelectric detectors. Chemical substitutions (e.g., A', A''; B', B'') are routinely used to modify properties. $(\text{Pb},\text{Sr})(\text{Zr},\text{Sn},\text{Ti})\text{O}_3$ and $(\text{Pb},\text{La})(\text{Zr},\text{Ti})\text{O}_3$ are typical compositions used in the piezoelectric and electrooptic ceramic industries.² Thus, PbTiO_3 -based materials are important for energy sensing and transducing applications and information storage and transmitting devices.

Recently, a powderless method of ceramic processing has evolved for the deposition of electrical ceramics in thin-layer form.³ The method is based upon polymeric sol-gel processing, where the constituents are mixed in solution before hydrolysis and condensation reactions form molecular linkages, with extended networks, and eventual gel formation. The solution method allows for a greater control of purity and mixing and, possibly, stoichiometry and homogeneity than is possible by conventional mixed-oxide powder processing. In addition, the method opens up new opportunities for the fabrication of electrical ceramics in a wide variety of shapes and forms (e.g., spin casting of $\text{Pb}(\text{Zr},\text{Ti})\text{O}_3$ coatings,⁴ drawing of PbTiO_3 fibers,⁵ etc.).

Lead titanate, PbTiO_3 , is a tetragonal ($4mm$) perovskite at room temperature.^{1,2} It is the only stable, low-temperature compound, in the $\text{PbO}-\text{TiO}_2$ system.⁶ A metastable monoclinic PbTi_3O_7 has been reported above 650 °C, which decomposes into PbTiO_3 and TiO_2 in the rutile form at higher temperatures.⁷ For tetragonal PbTiO_3 , a polar–nonpolar ($m3m$) transforma-

tion occurs on heating at 490 °C, and the tetragonal distortion becomes so large on cooling ($c/a = 1.06$ at 25 °C) that crack-free ceramics are difficult to form,² especially by high-temperature sintering of powders (e.g., 1200 °C).¹ Numerous additives (e.g., A', A'' = Sr, La; B', B'' = Zr, Sn, etc.) are used to reduce the tetragonal distortion and control properties for the industrial manufacture of crack-free insulators.²

Budd and co-workers demonstrated that pure PbTiO_3 coatings could be densified from a powder-free method at greatly reduced temperatures.⁸ The chemical sol-gel method was sufficiently reactive that spin-cast layers were dense and amorphous at 300 °C and crystallized into the perovskite structure by 425 °C.⁹ Low-temperature crystallization gives rise to nanocrystalline material in submicron layers. The starting materials were lead acetate trihydrate ($\text{Pb}(\text{OAc})_2 \cdot 3\text{H}_2\text{O}$), titanium isopropoxide ($\text{Ti}(\text{OPr}^i)_4$), and 2-methoxyethanol (2-MOE), and the synthesis procedures have been reported elsewhere.^{8–10} Subsequent investigations have attempted to identify the nature of the hydrolyzed lead titanate precursor, both in solution and in dried gels.¹¹

Prior to this study little information was available regarding the structure of heterometallic precursors in the $\text{Pb}(\text{OAc})_2-\text{Ti}(\text{OR})_4$ system.¹² One of our previous studies with 2-MOE produced an oily product which was unsuitable for crystallographic characterization.^{11c} In the present work, a bimetallic lead titanium alkoxide–acetate complex was isolated from an ethanolic PbTiO_3 precursor solution with a 1:1 $\text{Pb}(\text{OAc})_2:\text{Ti}(\text{OEt})_4$ ratio, and it was characterized by a single-crystal X-ray diffraction study, in addition to spectroscopic methods and chemical analysis.¹³ The new complex has a Pb:Ti ratio of 1:2, which is different from the composition of

(8) Budd, K. D.; Dey, S. K.; Payne, D. A. *Proc. Br. Ceram. Soc.* **1985**, *36*, 107.

(9) Schwartz, R. W.; Payne, D. A. In *Better Ceramics Through Chemistry III*; Brinker, C. J., Clark, D. E., Ulrich, D. R., Eds.; Materials Research Society: Pittsburgh, PA, 1988; p 199.

(10) Lakeman, C. D. E.; Payne, D. A. *J. Am. Ceram. Soc.* **1992**, *75*, 3091.

(11) (a) Li, S.; Condrate, Sr., R. A.; Spriggs, R. M. *Spectrosc. Lett.* **1988**, *21*, 969. (b) Dekleva, T. W.; Hayes, J. M.; Cross, L. E.; Geoffroy, G. *J. Am. Ceram. Soc.* **1988**, *71*, C-280. (c) Ramamurthi, S. D.; Payne, D. A. *J. Am. Ceram. Soc.* **1990**, *73*, 2547.

(12) (a) Caulton, K. G.; Hubert-Pfalzgraf, L. G. *Chem. Rev.* **1990**, *90*, 969. (b) Since the completion of this work (see: Chae, H. K.; Payne, D. A.; Z. Xu; Day, V. W. In *Abstracts of the 94th Annual Meeting of the American Ceramic Society, Minneapolis, MN*; American Ceramic Society: Westerville, OH, 1992; p 93), several groups have mentioned the syntheses of lead titanium acetatoalkoxides. (c) $[\text{PbTi}_2(\text{O})(\text{OOCCH}_3)(\text{OCH}_2\text{CH}_3)_7]_2$ was reportedly synthesized from $\text{Pb}_4\text{O}(\text{OAc})_6 \cdot \text{H}_2\text{O}$ and $\text{Ti}(\text{OPr}^i)_4$ with a Pb:Ti ratio of 1:1 in EtOH. See: Chandler, C. D.; Roger, C.; Hampden-Smith, M. J. *Chem. Rev.* **1993**, *93*, 1205. (d) Papiernik, R.; Hubert-Pfalzgraf, L. G.; Chaput, F. *J. Non-Cryst. Solids* **1992**, *147*, 148, 36. (e) Hubert-Pfalzgraf, L. G.; Boulmaaz, S.; Daniele, S.; Papiernik, R. In *Abstracts of the 7th International Workshop on Glasses and Ceramics from Gels*; Livage, J.; Babonneau, F.; Sanchez, C., Eds.; Paris, France, 1993; Abstract No. A3, to be published in *J. Sol-Gel Sci. Technol.* (f) Bates, J.; Zhang, Q.; Spiccia, L.; West, B. O. *Ibid.*, Abstract No. A6.

(13) Anal. Calcd for $\text{Pb}_2\text{Ti}_4\text{C}_{32}\text{H}_{76}\text{O}_{26}$: C, 27.71; H, 5.52; Pb, 29.88; Ti, 13.81. Found: C, 27.52; H, 5.44; Pb, 29.64; Ti, 14.11. IR (Nujol mull, cm^{-1}) 1565 (s), 1438 (s), 1373 (s), 1352 (m), 1134 (s), 1098 (s), 1059 (s), 924 (m), 898 (s), 722 (w), 665 (m), 594 (s), 509 (s), 453 (s). ¹H NMR (benzene-*d*₆, 20 °C) δ 4.91 (q, 4 H, OCH_2CH_3 , $J_{\text{H-H}} = 7$ Hz), 4.69 (q, 4 H, OCH_2CH_3 , $J_{\text{H-H}} = 7$ Hz), 4.55 (q, 4 H, OCH_2CH_3 , $J_{\text{H-H}} = 7$ Hz), 4.47 (q, 2 H, OCH_2CH_3 , $J_{\text{H-H}} = 7$ Hz), 2.01 (s, 3 H, OOCCH_3), 1.55 (t, 6 H, OCH_2CH_3 , $J_{\text{H-H}} = 7$ Hz), 1.48 (t, 3 H, OCH_2CH_3 , $J_{\text{H-H}} = 7$ Hz), 1.31 (t, 12 H, OCH_2CH_3 , $J_{\text{H-H}} = 7$ Hz). ¹³C NMR (benzene-*d*₆, 20 °C) δ 178.00 (s, OOCCH_3), 70.75 (s, OCH_2CH_3), 68.73 (s, $\text{OC}^i\text{H}_2\text{CH}_3$), 68.55 (s, $\text{OC}^o\text{H}_2\text{CH}_3$), 68.16 (s, $\text{OC}^o\text{H}_2\text{CH}_3$), 24.27 (s, OOCCH_3), 19.97 (s, OCH_2CH_3), 19.75 (s, OCH_2CH_3), 19.52 (s, OCH_2CH_3), 19.10 (s, OCH_2CH_3).

(1) Moulson, A. J.; Herbert, J. M. *Electroceramics: Materials, Properties and Applications*; Chapman and Hall: London, 1990; Chapter 5.

(2) Jaffe, B.; Cook, W. R.; Jaffe, H. *Piezoelectric Ceramics*; Academic Press: London, 1971; Chapter 6.

(3) See: *Ferroelectric Thin Films I, II, and III*; Materials Research Society: Pittsburgh, PA, 1990, 1992, 1993; Vols. 200, 243, and 310.

(4) Uhlmann, D. R.; Teowee, G.; Boulton, J. M.; Motakef, S.; Lee, S. C. *J. Non-Cryst. Solids* **1992**, *147*, 148, 409.

(5) Kamiya, K. In *Sol-Gel Optics: Processing and Applications*; Klein, L. C., Ed.; Kluwer Academic Publishers: Norwell, MA, 1994; p 126.

(6) See the binary phase diagram of $\text{PbO}-\text{TiO}_2$ in: *Phase Diagrams for Ceramists Volume VI*; Roth, R. S., Dennis, J. R., McMurdie, H. F., Eds.; American Ceramic Society: Westerville, OH, 1987; pp 135–136.

(7) Aykan, K. *J. Am. Ceram. Soc.* **1968**, *51*, 577.

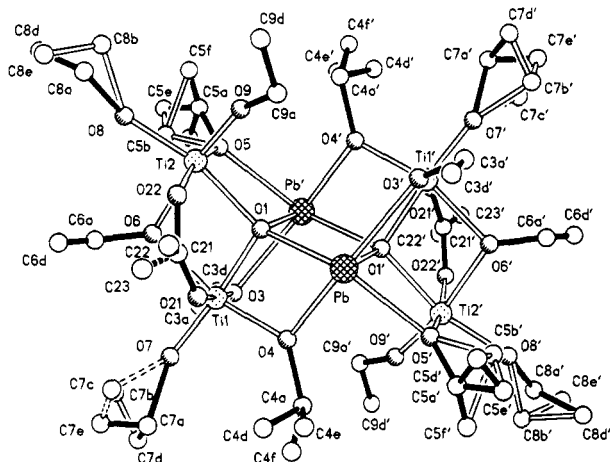


Figure 1. Perspective drawing of the non-hydrogen atoms in $[\text{PbTi}_2(\mu_4\text{-O})(\text{OOCCH}_3)(\text{OCH}_2\text{CH}_3)_7]_2$. Atoms labeled with a prime are related to nonprimed atoms by the crystallographic inversion center at $(0, \frac{1}{2}, \frac{1}{2})$ in the unit cell.

the precursor solution. Subsequently the yield was maximized by reacting $\text{Pb}(\text{OAc})_2$ and $\text{Ti}(\text{OEt})_4$ in a 1:2 stoichiometry. We investigated a composition range from 1:1 to 1:5 and determined the 1:2 compound to be the only isolable species. An optimized synthetic procedure is described as follows: Addition of $\text{Ti}(\text{OEt})_4$ (2.60 mL, 12.4 mmol) to anhydrous $\text{Pb}(\text{OAc})_2$ (1.99 g, 6.12 mmol) in dry EtOH (50 mL) yielded a colorless solution at room temperature. The solvent was removed by vacuum evaporation to produce a white powder. After 5 days at room temperature, transparent monoclinic crystals were obtained by recrystallization from diethyl ether to give $[\text{PbTi}_2(\text{O})(\text{OAc})(\text{OEt})_7]_2$ (2.18 g, 51.2% yield based on lead).

X-ray structural analysis of crystalline $[\text{PbTi}_2(\text{O})(\text{OAc})(\text{OEt})_7]_2$ revealed a dimeric structure (see Figure 1),¹⁴ which in principle is similar to that observed for $[\text{BaZr}_2(\text{OPr}^i)_{10}]_2$.¹⁵ Each half of the molecule consists of a basic triangular $\text{PbTi}_2(\mu_3\text{-O})$ unit with proper ligand attachments, and the two units are linked at the Pb and $\mu_3\text{-O}$ ions through the formation of a $\text{Pb}_2(\mu_4\text{-O})_2$ parallelogram as well as by $\mu_2\text{-OEt}$ ligands (vide infra). Within each monomeric unit, the Ti1–Ti2 base of the triangle is spanned by a $\mu_2\text{-OEt}$ and a $\mu_2\text{-OAc}$ group,

(14) Crystal structure was determined by Crystalitics Co., Lincoln, NE. The sample crystal ($0.35 \times 0.40 \times 0.40$ mm) was sealed inside a thin-walled glass capillary. The crystal is, at 20 ± 1 °C, monoclinic, space group $P2_1/n$ (an alternate setting of $P2_1/c-C^{52}_h$ (No. 14)) with $a = 14.398$ (3) Å, $b = 12.080$ (3) Å, $c = 17.007$ (4) Å, $\beta = 111.64$ (2)°, $V = 2749$ (1) Å³, and $Z = 2$ (formula units) $\{d_{\text{calc}} = 1.675$ g/cm³; μ_a (Mo $K\alpha$) = 6.75 mm⁻¹. A total of 3162 independent absorption-corrected reflections having 2θ (Mo $K\alpha$) < 43.0° (the equivalent of 0.5 limiting Cu $K\alpha$ spheres) were collected on a computer-controlled Nicolet autodiffractometer using full (1.00° wide) ω scans and graphite-monochromated Mo $K\alpha$ radiation. The structure was solved using "heavy atom" Patterson techniques with the Siemens SHELXTL-PLUS software package as modified at Crystalitics Company. The resulting structural parameters have been refined to convergence $\{R(\text{unweighted, based on } F) = 0.056$ for 1361 independent absorption-corrected reflections having 2θ (Mo $K\alpha$) < 43.0° and $I > 3\sigma(I)\}$ using counter-weighted full-matrix least-squares techniques and structural model which incorporated anisotropic thermal parameters for Pb, Ti, O, and nondisordered C atoms and isotropic thermal parameters for all disordered carbon atoms. The acetate ligand and several of the ethyl groups appear to be disordered in the lattice: atoms C₂₂, C₂₃, C_{4d}, C_{4e}, C_{4f}, C_{5a}, C_{5b}, C_{5d}, C_{5e}, C_{5f}, C_{7a}, C_{7b}, C_{7c}, C_{7d}, C_{7e}, C_{8a}, C_{8b}, C_{8d}, and C_{8e} were included in the refinement with occupancies of 0.40, 0.60, 0.25, 0.45, 0.30, 0.60, 0.40, 0.40, 0.35, 0.25, 0.33, 0.33, 0.33, 0.60, 0.40, 0.50, 0.50, 0.60, and 0.40, respectively.

(15) Vaartstra, B. A.; Huffman, J. C.; Streib, W. E.; Caulton, K. G. *Inorg. Chem.* **1991**, *30*, 3068.

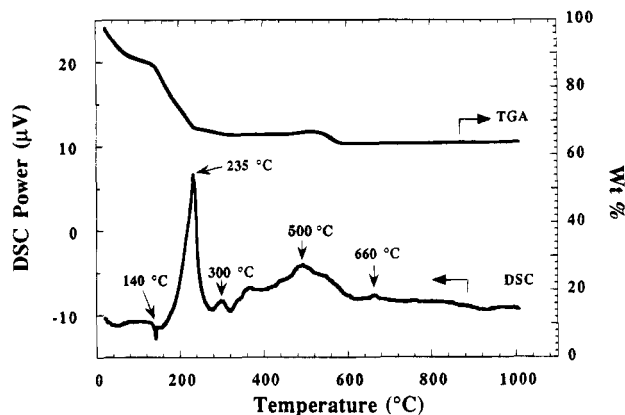


Figure 2. Thermal analysis of $[\text{PbTi}_2(\mu_4\text{-O})(\text{OOCCH}_3)(\text{OCH}_2\text{CH}_3)_7]_2$.

and three other -OEt ligands are associated with each Ti cation. However, no symmetry is observed for the triangle, as only the Ti1–Pb edge is connected by a $\mu_2\text{-OEt}$ ligand, leaving the Ti2–Pb edge unsupported. Two bridging Ti–O(Et)–Pb' linkages (Ti1–O3–Pb' and Ti–O5–Pb') also form for each $\text{PbTi}_2(\mu_4\text{-O})\text{-Pb}'$ assembly when the two halves are connected. Overall, each Ti cation has a hexacoordination with a distorted octahedral geometry. The average Ti–O distance is 1.975 Å (standard deviation $\sigma = 0.136$ Å) with an average *cis*-O–Ti–O angle of 89.7° ($\sigma = 7.4$ °). The coordination around Pb is five, with a pseudo-square-pyramidal configuration, attributed to interactions of bonding electron pairs with stereochemically active lone pair electrons on a Pb(II) center. Comparison with the cubic structure of PbTiO_3 ($m3m$) shows that the idealized Ti coordination environments are similar with coordination number (CN) six and symmetry of O_h , whereas the Pb cations have distinctively different environments (CN five vs twelve) and symmetries (C_s vs O_h) between the molecular species and the perovskite phase.

$[\text{PbTi}_2(\text{O})(\text{OAc})(\text{OEt})_7]_2$ was also characterized in solution by ^1H and $^{13}\text{C}\{^1\text{H}\}$ NMR spectroscopy in benzene- d_6 at ambient temperature. Besides the -OAc group, four chemically distinctive -OEt resonances with 2:2:2:1 ratio were observed in both the ^1H and ^{13}C NMR spectra, indicating the presence of a mirror symmetry in the molecule in solution.¹³ This requires changes in position of certain -OEt ligands which are inequivalent in the solid state.

The thermal decomposition of $[\text{PbTi}_2(\text{O})(\text{OAc})(\text{OEt})_7]_2$ crystals in air was examined by thermogravimetric analysis (TGA), differential scanning calorimetry (DSC), Fourier-transformed infrared spectroscopy (FT-IR), X-ray powder diffraction (XRD), and scanning electron microscopy (SEM) with energy-dispersive X-ray analysis (EDXA), as is relevant to the understanding of the evolution of structure in the formation of ceramic dielectrics. Figure 2 illustrates the TGA and DSC characteristics in air, and Figure 3 gives the FT-IR spectra after heat-treatment at various temperatures. The initial weight loss (Figure 2) below 140 °C can probably be attributed to the evaporation of alcohol formed by alkoxide ligand exchange with moisture, and the second weight loss between 140 and 300 °C was associated with a broad exothermic reaction, which was attributed to the thermolysis of alkoxy and acetate ligands. A further weight loss between 520 and 580 °C

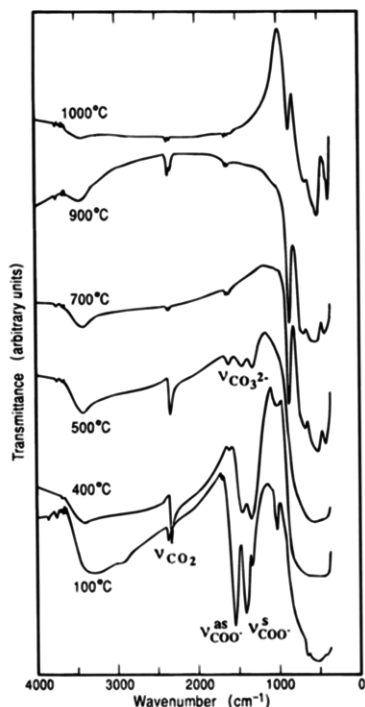


Figure 3. Room temperature Fourier-transformed infrared spectra for materials heat treated at the temperatures indicated.

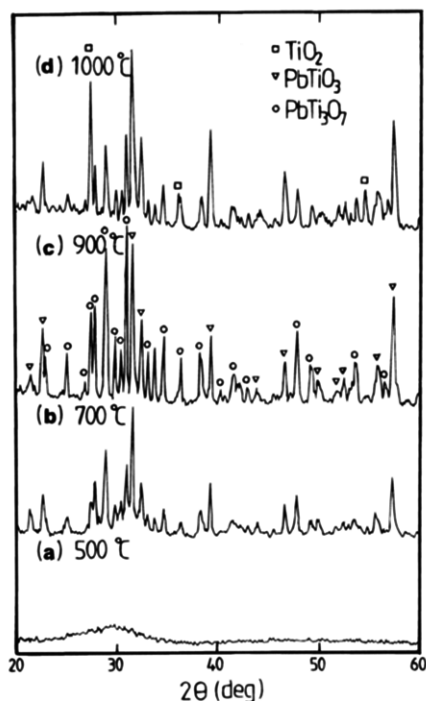


Figure 4. Room-temperature X-ray powder diffraction data for the thermal decomposition of $[\text{PbTi}_2(\mu_4\text{-O})(\text{OOCCH}_3)(\text{OCH}_2\text{-CH}_3)_7]_2$ at (a) 500, (b) 700, (c) 900, and (d) 1000 °C. New diffraction peaks (\square) appeared, and can be assigned to TiO_2 (rutile) patterns.

(Figure 2) was attributed to the decomposition of residual carbonate species (Figure 3) which formed in the solid state from acetate group decomposition products. Finally, the exotherm at 650 °C was associated with crystallization behavior. XRD data in Figure 4 indicates the material was amorphous to XRD after heat treatment at 500 °C for 1 h. Crystallization had started by 700 °C, and the material was a mixture of PbTi_3O_7

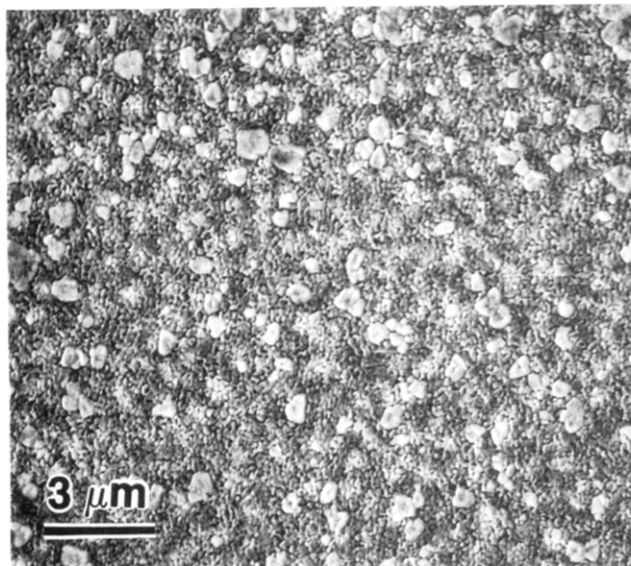


Figure 5. Scanning electron photomicrograph of a thin-layer deposited on platinumized silicon and heat treated at 700 °C.

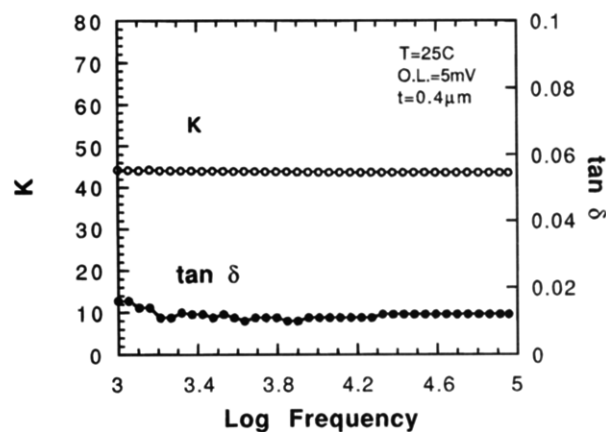


Figure 6. Dielectric properties as a function of frequency for a thin-layer capacitor integrated on silicon.

and PbTiO_3 at 900 °C. The intensities for the PbTi_3O_7 diffractions apparently decreased above 1000 °C, indicating the progressive decomposition of PbTi_3O_7 into PbTiO_3 and TiO_2 .

Thin layers were obtained by a metalloorganic decomposition method by spin casting a solution of the bimetallic complex onto platinumized silicon substrates followed by thermolysis.¹⁶ The layers were found to be dense and amorphous after heat treatment at 500 °C. Thermal processing at higher temperatures gave a crystalline mixture of PbTi_3O_7 and PbTiO_3 .⁷ Figure 5 shows a SEM photomicrograph of a layer crystallized at 700 °C and illustrates the heterogeneous nature of the ceramic microstructure. EDXA determined the fine-grain matrix ($<0.3 \mu\text{m}$) was richer in Ti than the larger dispersed phase ($0.5\text{--}1 \mu\text{m}$). The results are consistent with a PbTiO_3 phase dispersed within a PbTi_3O_7 matrix. The layers were dense and insulating as determined by dielectric measurements. Figure 6 gives the frequency dependence of dielectric properties for an integrated capacitor on silicon at 25 °C and 5 mV_{ac}. The $0.4 \mu\text{m}$

(16) The concentration of the bimetallic precursor dissolved in ethanol was 0.14 M. After each deposition, the layer was heat-treated at 300 °C for 1 min. The final assembly was crystallized at 700 °C in air for 1 h.

thick capacitor had stable dielectric properties between 1 and 100 kHz, with low values of $\tan \delta = 0.01$ and with a composite dielectric constant (\bar{K}) of 45. The two-phase mixture may find application in temperature-compensating capacitors.

Acknowledgment. The research was supported by the U.S. Department of Energy under Contract DMS-DEFG02-91ER45439. We acknowledge the use of facilities and services in the Molecular Spectroscopy Laboratory and the Microanalytical Laboratory of the School

of Chemical Sciences and in the Center for Microanalysis of Materials in the Materials Research Laboratory, at the University of Illinois. Technical help from Mr. M. A. Gulgun and the continued interest of Professor W. G. Klemperer are acknowledged.

Supplementary Material Available: Tables of atomic coordinates, anisotropic thermal parameters, bond lengths, and bond angles (8 pages); a listing of observed and calculated structure factors (3 pages). Ordering information is given on any current masthead page.